



**HAL**  
open science

## Sound velocity and refractive index of pure N<sub>2</sub> fluid and of equimolar N<sub>2</sub> –CO<sub>2</sub> fluid mixture up to 15 GPa

S. Ninet, Frédéric Datchi, G. Weck, A. Dewaele, P. Loubeyre, V. Giordano

### ► To cite this version:

S. Ninet, Frédéric Datchi, G. Weck, A. Dewaele, P. Loubeyre, et al.. Sound velocity and refractive index of pure N<sub>2</sub> fluid and of equimolar N<sub>2</sub> –CO<sub>2</sub> fluid mixture up to 15 GPa. *The Journal of Chemical Physics*, 2020, 153 (11), pp.114503. 10.1063/5.0021678 . hal-02954826

**HAL Id: hal-02954826**

**<https://hal.science/hal-02954826>**

Submitted on 16 Nov 2020

**HAL** is a multi-disciplinary open access archive for the deposit and dissemination of scientific research documents, whether they are published or not. The documents may come from teaching and research institutions in France or abroad, or from public or private research centers.

L'archive ouverte pluridisciplinaire **HAL**, est destinée au dépôt et à la diffusion de documents scientifiques de niveau recherche, publiés ou non, émanant des établissements d'enseignement et de recherche français ou étrangers, des laboratoires publics ou privés.

# Sound velocity and refractive index of pure N<sub>2</sub> fluid and of equimolar N<sub>2</sub>-CO<sub>2</sub> fluid mixture up to 15 GPa

S. Ninet\* and F. Datchi

*Institut de Minéralogie, de Physique des Matériaux et de Cosmochimie (IMPMC),  
Sorbonne Université, CNRS UMR 7590,  
IRD UMR 206, MNHN, 4, place Jussieu, Paris, France*

G. Weck, A. Dewaele, and P. Loubeyre  
*CEA, DAM, DIF, F-91297 Arpajon, France*

V. M. Giordano  
*Institut Lumière Matière, UMR 5306 Université Lyon 1-CNRS,  
F-69622 Villeurbanne Cedex, France*

(Dated: August 25, 2020)

## Abstract

The sound velocity and refractive index of pure N<sub>2</sub> and of equimolar N<sub>2</sub>-CO<sub>2</sub> mixture are measured up to 15 GPa and 700 K in a resistive heating Diamond Anvil Cell (DAC). The refractive index versus pressure is obtained by an interferometric method. The adiabatic sound velocity is then determined from the measurement of the Brillouin frequency shift in the backscattering geometry and the refractive index data. No phase separation of the N<sub>2</sub>-CO<sub>2</sub> fluid mixture is observed. The fluid mixture properties are discussed in terms of ideal mixing.

---

\* sandra.ninet@sorbonne-universite.fr

## I. INTRODUCTION

The properties of dense fluids of  $N_2$ ,  $CO_2$  and their mixtures, up to few 10 GPa pressures, are relevant for many questions such as the description of Neptune-like planetary interiors[1] and the decomposition of explosive materials[2]. The high pressure behaviour of  $N_2$ - $CO_2$  mixture are also important for the description of earth interior as fluid  $N_2$  and  $CO_2$ , mostly produced by sediments buried in subduction or collision zones, circulate in the deep crust [3], sometimes mixed [4, 5]. They interact with surrounding rocks under conditions reaching several GPa and  $\sim 800$  K. The physical and chemical properties of their mixtures are thus relevant to understand deep carbon and nitrogen cycles. Dense  $N_2$ - $CO_2$  fluid mixtures are also interesting from a fundamental point of view. At a first level of approximation, interactions in fluids  $N_2$  and  $CO_2$  can be described using very similar molecular effective diameter (differing by less than 6% [6]) which should favor their miscibility under pressure. However,  $N_2$  and  $CO_2$  molecules exhibit both a quadrupole moment, a moderate one  $-4.7(3) \cdot 10^{-40}$  C.m<sup>2</sup> for  $N_2$  and a large one  $-13.4 \cdot 10^{-40}$  C.m<sup>2</sup> for  $CO_2$  [7] associated to a large anisotropy of the  $CO_2$  pair interaction. Both effects should favor phase separation. The fluid-fluid miscibility is debated with calculations showing immiscibility[8] but not confirmed by other calculations[9]. In the dense  $N_2$ - $CO_2$  fluid mixtures, specifically along the melting line where entropy contribution, that favors miscibility, is minimum, the miscibility issue remains unexplored experimentally.

The properties of  $N_2$ - $CO_2$  fluids were mostly measured, more than 40 years ago, using piston-cylinder press, and hence have been limited to below 1-2 GPa [10–12]. The first measurements above 2 GPa was performed on the equimolar  $N_2$ - $CO_2$  mixture at 400 K up to 5 GPa in the the diamond anvil cell [13]. Complete miscibility was reported. Equation of state of dense fluid  $CO_2$  was measured combining a resistively heated DAC and Brillouin spectroscopy in the P-T range of 0.1–8 GPa and 300–700 K [14]. On the other hand, there are few data for pure  $N_2$  reported in the literature : Brillouin data collected at low and ambient temperature have been reported up to 0.5 GPa[15], the determination of the refractive index of  $N_2$  has been measured up to 1.7 GPa [12] and the sound velocity only up to 2.2 GPa[11] at 300 K.

Here, we report DAC measurements of the adiabatic sound velocity and of the refractive index in an equimolar  $N_2$ - $CO_2$  mixture up to 15 GPa and 700 K. The sound velocity  $v_s$  data are extracted by combining the refractive index  $n$ , determined by interferometric techniques, and the product  $nv_s$  measured by Brillouin scattering. To question the approximation of ideal mixing for dense  $N_2$ -

CO<sub>2</sub> fluids, we have also determined the same properties (refractive index and sound velocity) for pure fluid nitrogen up to 12 GPa and 700 K as these fundamental data were missing in literature.

## II. EXPERIMENTAL METHODS

The experiments were conducted in a membrane diamond anvil cell (mDAC). The N<sub>2</sub> and N<sub>2</sub>-CO<sub>2</sub> mixture (50.4 % moles of N<sub>2</sub>) were loaded in the sample chamber of the DAC under 1400 bar in a high pressure vessel. Rhenium was used as the gasket material. Pressure was measured from the ruby luminescence line at ambient temperature and from the SrB<sub>4</sub>O<sub>7</sub>:Sm<sup>2+</sup> one up to 700 K, using the calibrations given in Ref. [16]. The pressure uncertainty is 0.05 GPa at 300 K and 0.1 GPa at 700 K.

High temperatures were coupled to high pressures by putting the mDAC into a cylinder-shaped heater perfectly envelopping the cell. The temperature of the sample was measured using a K-thermocouple fixed on the head of one diamond anvil. Doing so, the temperature could be regulated within  $\pm 1$  K and the temperature uncertainty was estimated less than 5 K, as validated by previous studies[14, 17–19].

The adiabatic sound velocity of a fluid under high pressure in a DAC can be measured using Brillouin spectroscopy[20]. Without the knowledge of the refractive index, the sound velocity can be extracted by using several scattering geometries (for example backscattering and platelet geometries) or by working in the 90 scattering geometry[21]. This combination of Brillouin measurements or the use of a specific geometry, experimentally difficult to control, usually leads to a decrease of the accuracy in the sound velocity measurement. If the refractive index under pressure is accurately known, performing the Brillouin measurement in the backscattering geometry is thus generally selected to achieve the most accurate sound velocity measurements, as done in the present study. Brillouin spectra were obtained using a 6-pass Sandercock tandem Fabry-Perot[22], with a 514.5 nm laser line excitation. The Brillouin shift, denoted  $\Delta\sigma$ , is given by:

$$\Delta\sigma = 2 \frac{nv_s}{\lambda_0 c_0}, \quad (1)$$

where  $v_s$  is the acoustic phonon velocity,  $n$  is the refractive index,  $\lambda_0$  and  $c_0$  are respectively the incident wavelength and the velocity of the light in the vacuum.

The refractive index of the fluid was measured with the interferometric method described in Refs. [23 and 24]. It uses a combination of two types of optical interference created in the Fabry-

Perot cavity formed by the two parallel culets of both diamond anvils closing the sample chamber. The interference patterns obtained by illuminating the sample with a parallel white light beam allow measuring the product  $n \times t$  ( $t$  sample thickness) on one hand. On the other hand, convergent monochromatic light ( $\lambda=632.8$  nm) produces interference rings from which, with the input of  $n \times t$ , both thickness  $t$  and refractive index  $n$  of the sample are obtained. An uncertainty of  $\pm 0.5\%$  is typically achieved using this interferometric determination[24] in large part due to the strain of diamond anvil culets during the high pressure operation which affects interference rings radius.

### III. RESULTS ON PURE N<sub>2</sub>

#### A. Refractive index

Refractive index measurements of pure nitrogen have been performed from 0.06 to 7.5 GPa along 4 isotherms at 298K, 443 K, 489 K and 538 K. Most of the data have been collected by decreasing pressure, because, in that case, the Fabry-Perot cavity is of better quality due to reduced strain in the diamond anvils compared to those on pressure increase. The measured data points are presented in table I of the supplementary materials [25]. In the inset of figure 1, the N<sub>2</sub> refractive index is plotted versus pressure with a temperature color scale. A temperature shift is clearly seen. The evolution of the N<sub>2</sub> refractive index as a function of the pressure at ambient temperature will be useful for analyzing further measurements on dense fluid N<sub>2</sub>, such as for Brillouin spectroscopy here below or for Doppler shock velocity measurements of laser shock[26] in pre-compressed N<sub>2</sub> DAC targets. So the fit of the 296 K N<sub>2</sub> refractive index values over the P range [0.16-2.51 GPa] (at  $\lambda=632.8$  nm) is specifically given :

$$n_{N_2}(P) = a + b(1 + cP)^d \quad (2)$$

with the pressure  $P$  in GPa,  $a=0.62$ ,  $b=0.46$ ,  $c=19.0$  and  $d=0.112$ . A similar form of fit has already been used successfully for other molecular fluids [24].

Another useful representation of the change of the refractive index is through the Gladstone-Dale relation. It is the serie expansion of  $n-1$  versus the density change[27] and is expressed as  $n-1=K\rho$ . A modified version of the empirical Gladstone-Dale relation ( $n = a + K\rho$  with  $a$  closed to 1) is often used to fit the refractive index data under pressure up to few 10 GPa. We have used this formula in the present work. It was shown to work very well for several molecular systems such as He, Ne, H<sub>2</sub>, H<sub>2</sub>O[24] and, as shown below is working well also for N<sub>2</sub> and CO<sub>2</sub>. Taking

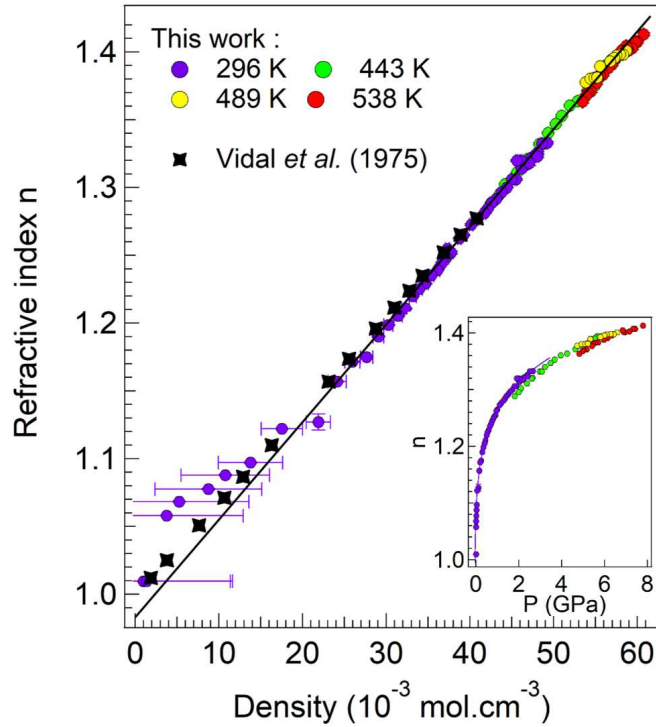


FIG. 1. (Color online) Refractive index of fluid  $N_2$  as function of the calculated density using the  $P(V)$  relation reported in Ref. [11] for different temperatures. The relative error bar on refractive index is generally smaller than 0.001. The relative error bar on density has been calculated by considering a relative error of  $\pm 0.025$  GPa. Our experimental data (circle) are compared to the ones reported in literature (black diamond) [12]. The black line corresponds to the linear fit of our experimental data (without the data at very low density i.e.  $< 20 \cdot 10^{-3} \text{ mol.cm}^{-3}$ ). The inset shows the evolution of the refractive index of  $N_2$  as function of the measured pressure at different temperatures.

into account the fluid  $N_2$  equation of state  $V = f(P, T)$  determined up to 2.2 GPa from 247 to 321 K [11], the  $n(P, T)$  data points are plotted versus density in figure 1. A linear dependence of the refractive index of fluid  $N_2$  with density is observed, independently of the temperature, following the relation:

$$n_{N_2}(\rho) = 0.9830(2) + 7.203(4)\rho, \quad (3)$$

with  $\rho$  in  $\text{mol.cm}^{-3}$

As can be seen in figure 1, the present data agree with the accurate values (based on capacitance measurements) collected up to  $0.04 \text{ mol.cm}^{-3}$  in Ref. 12, within experimental error bars, and extend the measurements of the refractive index to higher densities ( $0.061 \text{ mol.cm}^{-3}$ ). The

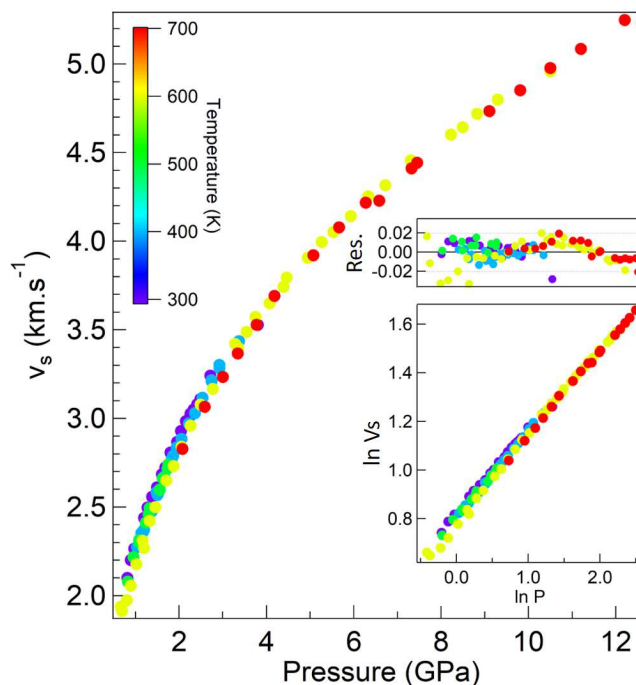


FIG. 2. (Color online) Evolution of the sound velocity  $v_s$  of fluid  $N_2$  as a function of the pressure (in GPa). Solid circles represent the present experimental data along 5 isotherms at 300 K, 400K, 500 K, 600 K and 700 K. The temperatures at which the data were collected are indicated by the color scale. Inset : Bottom : Logarithm representation of the evolution of the sound velocity ( $v_s$ ) of fluid  $N_2$  as a function of the pressure (in GPa). Top : residual from fit given by equation 4.

small deviation between the two data sets observed below  $0.015 \text{ mol.cm}^{-3}$  is ascribed to the large uncertainty in estimating the density in this range, as propagated from the pressure uncertainty (0.05 GPa).

### B. Adiabatic sound velocity

The Brillouin shift of pure  $N_2$  fluid as function of  $(P, T)$  has been measured along five isotherms - 300 K, 400 K, 500 K, 600 K and 700 K - up to 15 GPa. The  $nv_s(T, P)$  data points are listed in Table II of the SM[25]. The  $N_2$  adiabatic sound velocity is extracted from  $nv_s$  measurements using present refractive index determination. It is plotted versus pressure along the different isotherms in figure 2. As previously shown in pure  $CO_2$  [14], the pressure-temperature variation of the sound

velocity can be fitted with the following equation:

$$\ln v_s(P, T) = a + bT + c \ln P, \quad (4)$$

with the following parameters for pure N<sub>2</sub> :  $a=0.845(4)$ ,  $b=-0.000092(9)$  and  $c=0.3525(15)$  with  $v_s$  in km.s<sup>-1</sup>,  $T$  in K and  $P$  in GPa. This logarithm representation is shown in the inset of figure 2 : except at low pressure, the difference between data and fit by Eq. 4 is inferior to  $\pm 2\%$  (see top of the inset of figure 2).

#### IV. RESULTS ON N<sub>2</sub>-CO<sub>2</sub> EQUIMOLAR MIXTURE

##### A. Refractive index

The refractive index of N<sub>2</sub>-CO<sub>2</sub> fluid mixture has been measured along three isotherms - 300, 400 and 500 K - from 0.12 to 8.5 GPa. These data are reported in table III of the supplementary material [25] and Figure 3 shows the evolution of the refractive index of the equimolar fluid mixture as function of pressure for the different temperatures. We note that at 500 K, the fluid was preserved on compression up to 8.27 GPa and then solidification occurs : this is easily detectable since phase separation between N<sub>2</sub> and CO<sub>2</sub> is taking place. On decompression, we have shown that the homogeneous fluid is recovered below 5.16 GPa. The highest pressure measurement (8.27 GPa - 500 K) corresponds thus to a metastable fluid state.

At ambient temperature, the refractive index (at  $\lambda=632.8$  nm) has been measured in the fluid phase in the  $P$  range [0.12-0.88 GPa] (the liquidus pressure is 0.9 GPa) and these data can be fitted with the following equation :

$$n_{N_2-CO_2}(P) = a + b(1 + cP)^d \quad (5)$$

with the pressure  $P$  in GPa,  $a=-0.266$ ,  $b=1.382$ ,  $c=79.39$  and  $d=0.0313$ . The difference between the measurements and the fit is less than 1%.

As shown below, under the assumption of ideal mixing volume of fluids N<sub>2</sub> and CO<sub>2</sub>, the modified Gladstone-Dale relation is shown to perfectly reproduce this data set. Therefore, it somehow indicates that ideal mixing volume is a reasonable assumption in this dense N<sub>2</sub>-CO<sub>2</sub> equimolar fluid mixture.



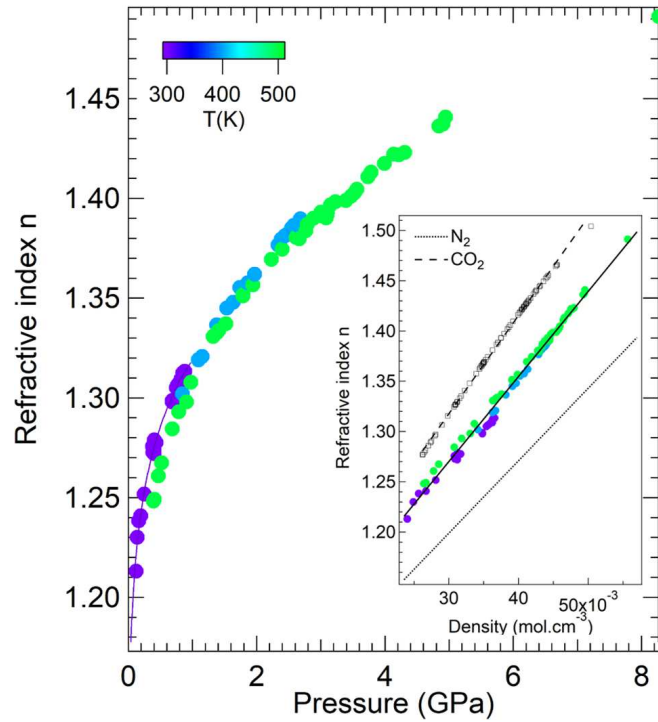


FIG. 3. (Color online) Evolution of the measured refractive index of equimolar  $N_2$ - $CO_2$  fluid with pressure along three isotherms (300, 400, 500 K). The temperatures at which the data were collected are indicated by the color scale. The symbols represent the data of the present work. The solid line corresponds to the fit of the data at 300 K. The inset shows the same refractive index data plotted as function of the calculated mixing density. The circles represent the equimolar  $N_2$ - $CO_2$  data and the solid line represents the linear fit. The squares represent the data of pure  $CO_2$  according to reference 14. Dotted and dashed represent the linear fit data of the data pure  $N_2$  (this work) and of pure  $CO_2$  ( $n_{CO_2} = 1.024(2) + 9.78(4)\rho_{CO_2}$ ) respectively.

### B. Adiabatic sound velocity

The Brillouin shift versus pressure in the  $N_2$ - $CO_2$  equimolar fluid has been measured along three isotherms - 300 K, 500 K and 700 K - up to 15 GPa. No evidence of phase separation was detected over this thermodynamic domain. The Brillouin data of  $nv_s$  are listed with pressure and temperature in table IV of the SM[25].

The adiabatic sound velocity of equimolar  $N_2$ - $CO_2$  fluid can be calculated directly using the present determination of the refractive index. We use the density linear fit of the refractive index versus ideal mixing density, as discussed above. The adiabatic sound velocity  $v_s$  of equimolar  $N_2$ - $CO_2$  mixture is plotted versus pressure for the different temperatures in figure 4(a). The error

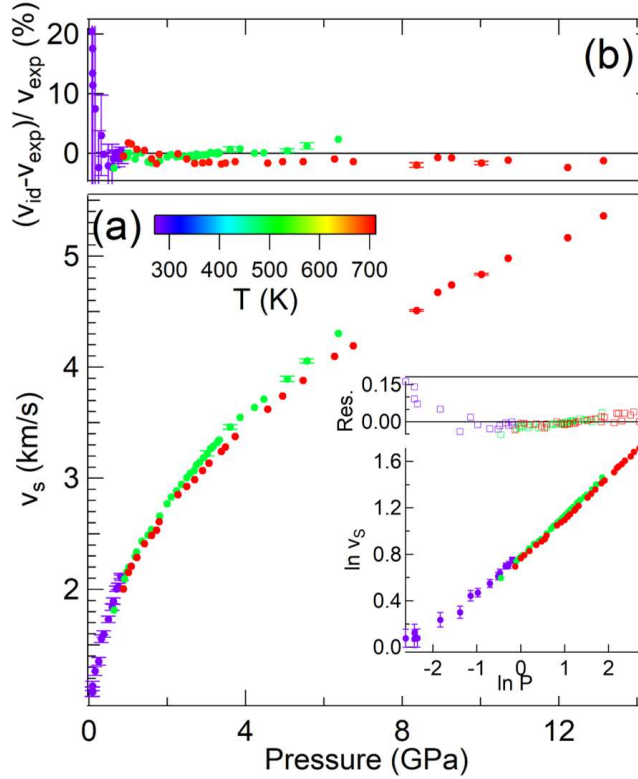


FIG. 4. (Color online) (a) Evolution versus pressure of the sound velocity in equimolar  $N_2$ - $CO_2$  fluid extracted from Brillouin scattering data in this work. The temperature at which the data were collected is indicated by the color scale. Inset : evolution of the logarithm of the sound velocity ( $\ln v_s$ ) of equimolar  $N_2$ - $CO_2$  fluid as a function of the logarithm Pressure (in GPa). Top : Residual from fit given by equation (5). (b) Relative deviation between our data and the ideal mixture model.

bars on the sound velocity, propagated from the pressure uncertainty, are around  $\pm 10\%$  at 0.1 GPa (see the inset) and below  $\pm 1\%$  at 15 GPa.

The inset of Figure 4(a) shows the evolution of the sound velocity as function of the pressure in a logarithm representation for the different temperatures. Except for the low pressure region ( $P < 0.3$  GPa) where the uncertainties on the sound velocity are large, our data of the sound velocities in  $N_2$ - $CO_2$  as function of the pressure are well fitted with the same fit function as in pure  $N_2$  or in pure  $CO_2$  [14] :

$$\ln v_s(P, T) = a + bT + c \ln P \quad (6)$$

with the following coefficients :  $a=0.851(18)$ ,  $b=-0.00010(4)$  and  $c=0.346(7)$  (with  $P$  in GPa and

$T$  in K).

## V. DISCUSSION

### A. Ideal mixing in N<sub>2</sub>-CO<sub>2</sub> mixture

The equation of state of N<sub>2</sub>-CO<sub>2</sub> fluid mixture is not available in the literature. Assuming the general validity of the Gladstone-Dale formula for molecular systems under pressure, the hypothesis of ideal mixing volume in the N<sub>2</sub>-CO<sub>2</sub> mixtures can be tested. Ideal mixing density of the N<sub>2</sub>-CO<sub>2</sub> mixture is given by :

$$\rho(P, T) = \left( \frac{x_1}{\rho_1} + \frac{x_2}{\rho_2} \right)^{-1} \quad (7)$$

where 1 and 2 refers to the pure components (N<sub>2</sub> and CO<sub>2</sub>),  $x_i$  are the molar fraction (here  $x_1 = x_2 = 0.5$ ) and  $\rho_i$  the density of the pure component  $i$  (for pure fluid CO<sub>2</sub> reported in reference [14] and for N<sub>2</sub> in reference [11]). The inset of figure 3 shows the evolution of the refractive index of the N<sub>2</sub>-CO<sub>2</sub> mixture as function of the calculated ideal mixing density. The following Gladstone-Dale relationship fits well the experimental data:

$$n(P, T) = 1.0165(3) + 8.459(8)\rho(P, T) \quad (8)$$

with  $\rho(P, T)$  in mol.cm<sup>-3</sup>. *Hence that strongly suggests that ideal mixing volume is operative in N<sub>2</sub>-CO<sub>2</sub> fluid mixtures in the few GPa pressure range.*

It is interesting to determine whether the measured adiabatic sound velocity can strengthen the evidence for an ideal mixture description for N<sub>2</sub>-CO<sub>2</sub> mixture. Therefore, the sound velocity  $v_s$  of the mixture is calculated by combining the additivity of the molar volume ( $V = V_1 + V_2$ ) and the thermodynamic definition of the adiabatic sound velocity, given by:

$$v_s^2 = -\frac{V^2}{M} \left( \frac{\partial P}{\partial V} \right)_S \quad (9)$$

where  $V$  is the molar volume,  $P$  is the pressure and  $M$  is the molar mass.

The sound velocity of the ideal mixture can then be straightforwardly expressed from the experimental data ( $V_i(P, T)$  and  $v_{si}(P, T)$ ) of the pure components as:

$$v_s^2 = \frac{(x_1 V_1 + x_2 V_2)^2}{x_1 M_1 + x_2 M_2} \left( \frac{x_1 V_1^2}{M_1 v_{s1}^2} + \frac{x_2 V_2^2}{M_2 v_{s2}^2} \right)^{-1} \quad (10)$$

where  $v_{si}$  are the sound velocity,  $V_i$  the molar volume and  $M_i$  the molar mass of the  $i$  component of the ideal mixture.

Ideal mixing calculation is so made using the equation of state of fluid CO<sub>2</sub> [14] and N<sub>2</sub> [11], the sound velocities of CO<sub>2</sub> [14] and of N<sub>2</sub>, as presented above. To be consistent with our experiment, in the case of CO<sub>2</sub>, we have used the values of the sound velocity measured by Brillouin scattering, so without considering frequency dispersion. A good agreement is obtained in figure 4(b) between the ideal mixing calculation and present data. At low pressure (below 0.2 GPa) though, a significant deviation seems to be observed (up to 20%), the measured sound velocity being higher than the calculated sound velocity. In fact, in this pressure range, as the relative uncertainty in  $P$  and thus in  $v_s$  are quite large, we can conclude that within the precision of our experiment, our measurements and the model are compatible at low pressure. We note that this low precision also exists for the data reported in the pure components, as discussed above for N<sub>2</sub>, and that increases further the uncertainty of the deviation. Above 0.4 GPa and up to 15 GPa, an excellent agreement between the ideal mixture model and present measurement is observed with a relative deviation less than 2% (see fig.4(b)). The ideal mixture is thus a good model to describe the equimolar N<sub>2</sub>-CO<sub>2</sub> mixture.

### B. Dispersion of the sound velocity in N<sub>2</sub>-CO<sub>2</sub> fluids

Brillouin frequencies are in the gigahertz range (5-33 GHz for the present work) whereas ultrasonic measurements are typically performed in the MHz. Dispersion of sound waves in molecular fluids have been the subject of investigations in the past and it is mainly understood in terms of relaxation of energy into internal (vibrational and rotational) degrees of freedom[30]. It is expected and observed in many polyatomic fluids that the positive dispersion characteristic of relaxation phenomena disappears by increasing density, as measured in fluid H<sub>2</sub>[31]. That is also observed here in fluid N<sub>2</sub>, see in figure 5(a), since the Brillouin data are, below 1.3 GPa, slightly higher than the ultrasonic measurements[11] but both measurements converge above. However, in pure CO<sub>2</sub>, the positive dispersion is observed up to 0.5 GPa at least[14]. The extension of ultrasonic measurements in fluid CO<sub>2</sub> in a higher pressure range is needed to observe the expected disappearance of the dispersion.

To our knowledge, there is no measurement of the ultrasound velocity of equimolar N<sub>2</sub>-CO<sub>2</sub> mixtures. Nevertheless, we can compare our present Brillouin data to the ones reported

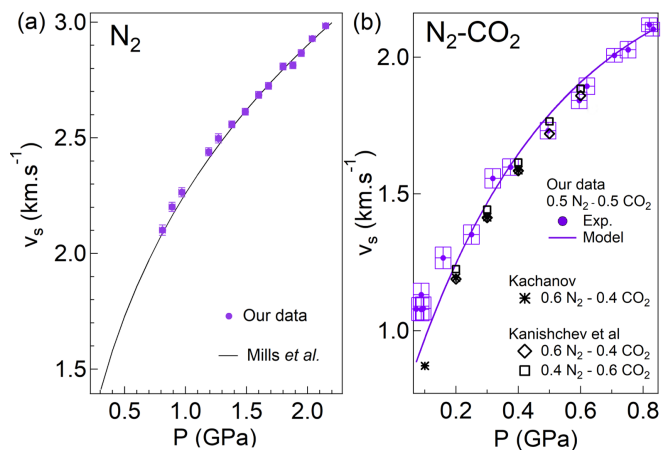


FIG. 5. (Color online) (a) Comparison between the present data of adiabatic sound velocity in pure  $\text{N}_2$  determined by Brillouin measurements (solid circle) and the ultrasonic measurements [11] (black solid line) at ambient temperature (b) Comparison between the present data of adiabatic sound velocity in  $\text{N}_2\text{-CO}_2$  mixture determined by Brillouin measurements (purple solid circle) and previous ultrasonic measurements [28, 29] (black symbols) at ambient temperature. The calculated adiabatic sound velocity is presented by the purple curve.

for ultrasonic measurements in  $\text{N}_2\text{-CO}_2$  mixtures of two different concentrations : a first mixture with 60.4% moles of  $\text{N}_2$  and 39.6% of  $\text{CO}_2$  [28, 29] and a second  $\text{N}_2\text{-CO}_2$  mixture with 39.4% moles of  $\text{N}_2$  and 60.6% of  $\text{CO}_2$  [29] from 0.1 to 0.6 GPa at ambient temperature. The ultrasonic sound velocity in the MHz frequency range of the equimolar  $\text{N}_2\text{-CO}_2$  mixture should thus be in between the values of these two concentrations. The comparison between these ultrasonic measurements and the present Brillouin data is made in figure 5(b). At low pressure, below 0.2 GPa, the Brillouin sound velocities are slightly higher (by  $\approx 10\%$  at 0.1 GPa) than the ones obtained by ultrasonic measurement, even if we consider the uncertainties on the sound velocities of our work. Above 0.3-0.5 GPa, present data becomes similar (considering the uncertainties) to the ones reported by ultrasonic measurements. Consequently, the dispersion either disappears or is too small to be resolved and so that the Brillouin velocity in the GHz can be used as the thermodynamic sound velocity.

## VI. CONCLUSIONS

The present work extends by one order of magnitude in pressure the measurements of the sound velocity and refractive index of dense fluids  $N_2$  and  $N_2$ - $CO_2$  equimolar mixture. The  $N_2$ - $CO_2$  mixture remains completely miscible up to 15 GPa, even for temperatures near the melting line. The analysis of the refractive index and of the sound velocity versus pressure suggests that the  $N_2$ - $CO_2$  equimolar mixture can be considered as ideal with properties directly deduced from volumic fraction of  $N_2$  and  $CO_2$  pure fluids. In pure  $N_2$  and in the  $N_2$ - $CO_2$  mixture, the dispersion of the sound velocity between Brillouin measurements (done in the GHz range) and the previous ultrasonic measurements (done in the MHz range) is no more resolved within the experimental accuracy above about 0.5 GPa.

## DATA AVAILABILITY STATEMENTS

The data that support the findings of this study are available from the corresponding author upon reasonable request.

## SUPPLEMENTARY MATERIALS

See the supplementary materials for the tables of the experimental data.

- 
- [1] T. Guillot and D. Gauthier, *Giant planets in "Treatise on Geophysics" (second edition)*, edited by T. Spohn and G. Schubert (Elsevier, 2015).
  - [2] V. Dubois, N. Desbiens, and J. Clerouin, *Journal of Applied Physics* **122**, 185902 (2017).
  - [3] R. Rudnik, ed., *The crust, Treatise on Geochemistry, Volume 3* (Elsevier, 2007).
  - [4] T. Andersen, H. Austrheim, E. Burke, and S. Elvevold, *Chemical Geology* **108**, 113 (1993).
  - [5] J. Touret, *Chemical Geology* **37**, 49 (1982).
  - [6] D. Ben-Amotz and D. R. Herschbach, *J. Phys. Chem.* **94**, 1038 (1990).
  - [7] C. Graham, J. Pierrus, and R. E. Raab, *Molecular Physics* **67**, 939 (1989), <https://doi.org/10.1080/00268978900101551>.
  - [8] A. Kreglewski and K. R. Hall, *Fluid Phase Equilibria* **15**, 11 (1983).

- [9] R. Thiery, A. VanDenKerkhof, and J. Debussy, *Eur. J. Mineral.* **6**, 753 (1994).
- [10] L. L. Pitaevskaya and A. V. Bilevich, *Russian Journal of Physical Chemistry* **47**, 126 (1973).
- [11] R. L. Mills, D. H. Liebenberg, and J. C. Bronson, *J. Chem. Phys.* **63**, 1198 (1975).
- [12] D. Vidal and M. Lallemand, *J. Chem. Phys.* **64**, 4 (1976).
- [13] M. E. Kooi, J. A. Schouten, A. M. VanDenKerkhof, G. Istrate, and E. Althaus, *Geochimica et Cosmochimica Acta* **62**, 2837 (1998).
- [14] V. M. Giordano, F. Datchi, and A. Dewaele, *J Chem Phys* **125**, 054504 (2006).
- [15] H. D. Hochheimer, K. Weishaupt, and M. Takesadaba, *J. Chem. Phys.* **105**, 374 (1996).
- [16] F. Datchi, R. LeToullec, and P. Loubeyre, *J. Appl. Phys.* **81**, 3333 (1997).
- [17] F. Datchi, P. Loubeyre, and R. LeToullec, *Phys. Rev. B* **61**, 6535 (2000).
- [18] F. Datchi and B. Canny, *Phys. Rev. B* **69**, 144106 (2004).
- [19] S. Ninet and F. Datchi, *J Chem Phys* **128**, 154508 (2008).
- [20] M. Grimsditch and A. Polian, *Simple molecular systems at very high density*, edited by P. L. A. Polian and N. Boccara (Plenum, 1989).
- [21] C. H. Whitfield, E. Brody, and W. Basset, *Rev. Scien. Instruments* **47**, 942 (1976).
- [22] J. R. Sandercock, *U. S. Patent* **4**, 225 (1980).
- [23] R. LeToullec, P. Loubeyre, and J. P. Pinceaux, *Phys. Rev. B* **40**, 2368 (1989).
- [24] A. Dewaele, J. H. Eggert, P. Loubeyre, and R. LeToullec, *Phys. Rev. B* **67**, 94112 (2003).
- [25] "See supplementary materials of "sound velocity and refractive index of pure N<sub>2</sub> fluid and of equimolar N<sub>2</sub>-CO<sub>2</sub> fluid mixture up to 15 GPa" by S. Ninet and al."
- [26] S. Brygoo, M. Millot, P. Loubeyre, A. E. Lazicki, S. Hamel, T. Qi, P. M. Celliers, F. Coppari, J. H. Eggert, D. E. Fratanduono, D. G. Hicks, J. R. Rygg, R. F. Smith, D. C. Swift, G. W. Collins, and R. Jeanloz, *Journal of Applied Physics* **118**, 195901 (2015).
- [27] R. E. Setchell, *J. App. Phys.* **91**, 2833 (2002).
- [28] Y. L. Kachanov, Kanishchev, and L. L. Pitaevskaya, *Inzhenerno-Fizicheskii Zhurnal* **44**, 5 (1983).
- [29] B. E. Kanishchev, L. L. Pitaevskaya, and S. L. Gutman, *Dokl. Akad. Nauk SSSR* **257**, 1348 (1981).
- [30] K. F. Herzfeld and T. A. Litovitz, *Absorption and Dispersion of Ultrasonic Waves*, edited by H. Massey and K. Brueckner (Academic press, 1959).
- [31] G. Pratesi, L. Ulivi, F. Barocchi, P. Loubeyre, and R. L. Toullec, *J. Phys.: Condens. Matter* **9**, 10059 (1997).

Refractive index  $n$

